Monte Carlo Simulations of Liquid−Liquid Equilibria for Ternary Chain Molecule Systems on a Lattice

Jianwen Jiang, Qiliang Yan, Honglai Liu, and Ying Hu*

Thermodynamics Research Laboratory, East China University of Science and Technology, Shanghai 200237, China

Received December 19, 1996; Revised Manuscript Received September 30, 1997[⊗]

ABSTRACT: The configuration-bias-vaporization method developed previously for binaries is successfully extended to the simulation of liquid−liquid equilibria of ternary chain molecule systems based on a lattice. The effects of varying the chain lengths and interaction energies on the binodals are examined. Comparisons between simulation results and predictions of the Flory−Huggins theory and the Freed theory are also made. It is shown that the agreement is satisfactory when the compositions are near the corresponding binaries. The discrepancies become larger when the compositions approach the critical consolute point. Generally, the Freed theory gives better agreement than the Flory−Huggins theory. However, improvements are still needed to describe systems near the critical region for both binaries and ternaries.

1. Introduction

Recently, direct simulation of phase equilibria of fluids and polymers has made remarkable progress as illustrated by Panagiotopoulos et al.'s Gibbs ensemble method,[1] Laso et al.'s continuum-configurational-bias-Gibbs-ensemble method,[2] as well as by the works of Madden et al.,[3] Guo et al.,[4] and Mackie et al.[5] Employing these advances as well as Harris and Rice's[6] and Siepmann's[7] revised Rosenbluth−Rosenbluth procedure, we have developed a configuration-bias-vaporization method (CBV)[8] for direct molecular simulation of phase equilibria of polymer systems based on a lattice. Liquid−liquid equilibria of binary polymer solutions with polymer chain lengths varying from 1 to 200 have been obtained. Corresponding predictions using the classical Flory−Huggins theory[9] and Freed et al.'s modern lattice-cluster theory (LCT)[10,11] were also tested. The LCT theory is more rigorous and is formally an exact solution of the Flory−Huggins lattice method utilizing a sophisticated virial expansion. The comparisons show that the predictions of both theories for the coexisting curves are satisfactory if the temperature is not too high. As for the critical points, the LCT theory gives satisfactory critical temperatures while the Flory−Huggins theory shows larger discrepancies as expected. However, both theories predict the critical compositions poorly. In this work, we extend the CBV method to ternary chain molecule systems based on a lattice. Phase diagrams for systems with varying chain lengths and interaction energies are presented.

In the literature, little previous computer-simulation work has been reported for ternary chain molecule systems except some symmetrical ones in Sariban and Binder's[12−15] and Deutsch and Binder's[16] work, where all of the chain molecules $r_2 = r_3$ have equal chain lengths. Work on systems with $r_2 \neq r_3$ does not appear to have been reported. The present work is therefore focused on unsysmmetrical systems. As it is anticipated that molecular thermodynamic models will chiefly be used for the prediction of multicomponent phase equilibria using only the parameters for corresponding binaries, accurate computer-simulation results for ternaries are critically needed to test the reliability of such predictions. The present work can facilitate such testing. As examples we again test both the Flory−Huggins theory and the LCT theory using the present ternary computer-simulation results.

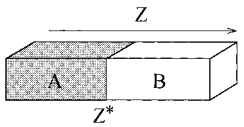

Figure 1. Schematic illustration of simulation box.

2. Simulation Method

Simulations are performed in a canonical ensemble. Linear chain-molecules are modeled by self-avoiding walks on a cubic lattice with a height much larger than its length and width. A typical size is 16 × 16 × 128. Periodic boundary conditions are used to eliminate the boundary effect. Solvent molecules with unit chain length $r_1 = 1$ are treated as holes. In this respect, the incompressible mixture of linear chain molecules and solvent is mapped onto a compressible lattice fluid of linear chain molecules at constant volume. Before initiation, we set two impenetrable plates with infinite area at $z = 0$ and $z = Z^*$. The whole system is separated into two compartments A and B as shown in Figure 1. We then randomly insert two kinds of chain molecules with chain lengths r_2 and r_3 into compartment A using the Rosenbluth−Rosenbluth growth method.[17] Soon after all the chain molecules have been inserted, the two plates are removed. All chain molecules can then move over the whole lattice. The condensed chain molecules in compartment A evaporate gradually into compartment B.

In the process of carrying out the simulation, five types of molecular motions are used. They are reptation (0.1), internal motion (0.1) including end-rotation, L-flip and crankshaft,[18] and the Rosenbluth−Rosenbluth growth method revised by Siepmann et al.[7] (0.8). Values in brackets are the corresponding selection probabilities. In the Rosenbluth−Rosenbluth growth method, we first arbitrarily remove a chain molecule from the system and select a position randomly as a new starting-point for growth. We then insert the removed chain molecule segment by segment. If the insertion is successful, we accept this new configuration according to the probability

$$p = \min \{1, w_{new}/w_{old}\} \quad (1)$$

where, w_{new} and w_{old} are, respectively, Rosenbluth factors before and after the chain is renewed. If the insertion fails, we return to the old configuration of the removed chain and

* To whom correspondence should be addressed.

[⊗] Abstract published in *Advance ACS Abstracts,* December 1, 1997.

S0024-9297(96)01873-6 CCC: $14.00

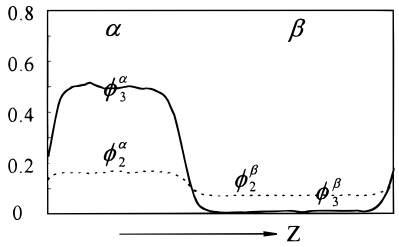

Figure 2. Segment density distribution at equilibrium.

Table 1. Model Parameters of Six Systems

system	r_1	r_2	r_3	$\tilde{\epsilon}_{12}$	$\tilde{\epsilon}_{13}$	$\tilde{\epsilon}_{23}$
1	1	4	16	0.250	0.500	−0.100
2	1	4	24	0.250	0.500	−0.100
3	1	4	32	0.250	0.500	−0.100
4	1	4	8	0.333	0.556	0.100
5	1	4	8	0.333	0.556	0.000
6	1	4	8	0.333	0.556	−0.200

attempt insertion again. Among these five types of motion, the first four move the chains locally, keeping them in a small region. The correlation between the old and new configurations is then relatively large. Fortunately, the efficiency of the fifth motion is higher owing to its larger degree of movement. Therefore, the Rosenbluth−Rosenbluth growth plays a predominant role in the simulation.

Segment densities are calculated every 1000 steps. After a long time, usually 10^8 trial moves, the whole system approaches the equilibrium state. If the initial composition is in the stable one-phase region, the final concentrations of the two kinds of chain molecules will be equal and homogeneous along the Z direction. On the contrary, if the initial composition is in the unstable two-phase region, two coexisting phases with different compositions will appear in the Z direction at the end of the simulation. The segment density along the Z direction is defined by

$$\phi_i = N_i/N_t \tag{2}$$

where N_i is the number of sites occupied by segments of chain molecules of kind i; N_t is the total number of lattice sites. The densities of the coexisting phases are obtained from the density profile directly.

Figure 2 shows typical distributions of segment densities of the two kinds of chain molecules along the Z direction. Two coexisting phases α and β with different compositions are clearly shown.

3. Results and Discussion

Using the simulation method described above, we have studied liquid−liquid equilibria in six systems. Their molecular parameters are shown in Table 1, where chain lengths r_i vary from 1 to 32, and reduced exchange interaction energies $\tilde{\epsilon}_{ij}$ vary from −0.200 to 0.556. $\tilde{\epsilon}_{ij}$ is defined by

$$\tilde{\epsilon}_{ij} = (\epsilon_{ii} + \epsilon_{jj} - 2\epsilon_{ij})/kT \tag{3}$$

where ϵ_{ij} is the interaction energy parameter between segments of component i and j. Binaries 1−2 and 2−3 are assumed to be miscible, while the binary 1−3 is partially miscible. Because we are dealing with a compressible lattice fluid of chain molecules at constant volume, the present work is restricted to upper-critical-solution-temperature (UCST) systems.

Table 2 lists the acceptance ratios of the configuration-bias growth for all six systems. The magnitude is about 10^{-2}. In 10^8 trial moves, around 10^6 effective moves actually take place, which is sufficient to yield an equilibrium state. A small decrease in the acceptance ratio is seen as the chain length r_3 increases.

Table 2. Acceptance Ratios

system	acceptance ratio	system	acceptance ratio
1	0.037	4	0.050
2	0.024	5	0.047
3	0.010	6	0.045

Table 3. Coexisting Compositions and Statistaical Uncertainties of System 1

ϕ_2^α	ϕ_3^α	ϕ_2^β	ϕ_3^β
0.077 ± 0.006	0.66 ± 0.05	0.052 ± 0.003	0.018 ± 0.003
0.100 ± 0.005	0.63 ± 0.03	0.072 ± 0.002	0.024 ± 0.002
0.130 ± 0.004	0.57 ± 0.02	0.096 ± 0.001	0.032 ± 0.001
0.146 ± 0.005	0.53 ± 0.02	0.110 ± 0.002	0.042 ± 0.001
0.167 ± 0.008	0.48 ± 0.04	0.131 ± 0.003	0.050 ± 0.005
0.188 ± 0.009	0.35 ± 0.07	0.170 ± 0.005	0.120 ± 0.007

Table 4. Simulation Results of Liquid−Liquid Equilibria

ϕ_2^α	ϕ_3^α	ϕ_2^β	ϕ_3^β	ϕ_2^α	ϕ_3^α	ϕ_2^β	ϕ_3^β
System 1							
0.077	0.66	0.052	0.018	0.146	0.53	0.110	0.042
0.100	0.63	0.072	0.024	0.167	0.48	0.131	0.050
0.130	0.57	0.096	0.032	0.188	0.35	0.170	0.120
System 2							
0.051	0.74	0.020	0.002	0.167	0.56	0.140	0.024
0.078	0.70	0.060	0.005	0.204	0.48	0.162	0.038
0.142	0.60	0.088	0.010	0.211	0.44	0.177	0.051
0.149	0.58	0.110	0.016	0.231	0.39	0.185	0.060
System 3							
0.023	0.77	0.019	0.003	0.158	0.58	0.087	0.009
0.060	0.72	0.025	0.004	0.220	0.48	0.136	0.017
0.083	0.68	0.042	0.005	0.239	0.44	0.190	0.030
0.118	0.64	0.083	0.008	0.280	0.33	0.241	0.059
System 4							
0.065	0.68	0.065	0.052	0.126	0.58	0.116	0.089
0.093	0.64	0.095	0.071	0.155	0.50	0.123	0.100
0.100	0.63	0.108	0.080	0.168	0.47	0.132	0.121
System 5							
0.054	0.70	0.022	0.041	0.185	0.48	0.080	0.067
0.090	0.64	0.036	0.049	0.220	0.40	0.100	0.061
0.120	0.60	0.047	0.050	0.236	0.33	0.112	0.078
0.150	0.55	0.062	0.055	0.191	0.21	0.115	0.080
System 6							
0.040	0.76	0.010	0.020	0.210	0.52	0.070	0.036
0.075	0.72	0.020	0.023	0.235	0.47	0.100	0.048
0.136	0.64	0.028	0.026	0.247	0.44	0.115	0.057
0.162	0.60	0.045	0.028	0.258	0.40	0.128	0.067

Table 3 shows compositions and corresponding statistical uncertainties for coexisting phases of system 1. The statistical uncertainty is slightly greater at lower temperature region and near the critical consolute point.

Numerical simulation results of liquid−liquid equilibria for all six systems are listed in Table 4.

For the series of systems 1, 2, and 3, reduced exchange interaction-energy parameters are kept as fixed. The chain length of component 3, r_3 is chosen as a variable to examine the effect of chain length on phase equilibria. Figures 3−5 show the resulting binodals from the computer simulations and those from the Flory−Huggins theory and LCT theory. The immiscible region becomes larger when the chain length of component 3 becomes longer as expected. The agreement between the simulation results and both theories is satisfactory when the compositions are near the corresponding binaries. The discrepancies become larger when the compositions approach the critical consolute point. As shown in the figures, the LCT theory gives better agreement than the Flory−Huggins theory. However, as we have shown in our previous work for

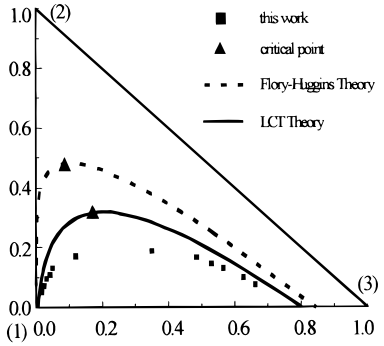

Figure 3. Liquid−liquid equilibria of system 1.

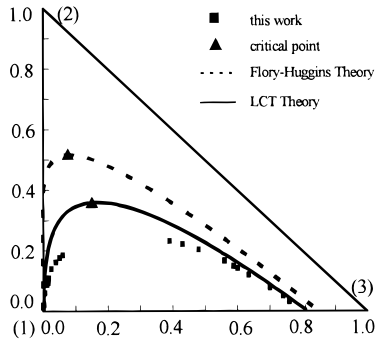

Figure 4. Liquid−liquid equilibria of system 2.

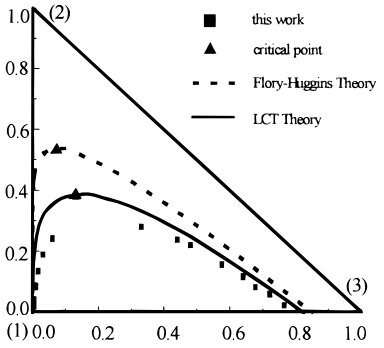

Figure 5. Liquid−liquid equilibria of system 3.

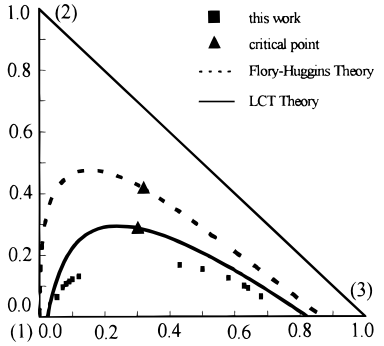

Figure 6. Liquid−liquid equilibria of system 4.

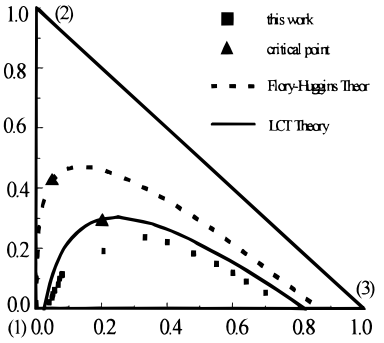

Figure 7. Liquid−liquid equilibria of system 5.

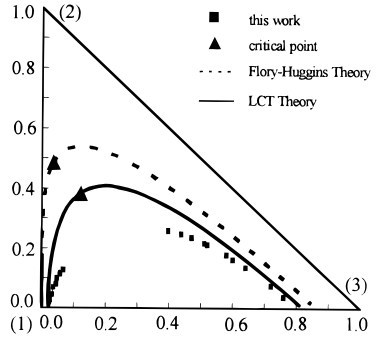

Figure 8. Liquid−liquid equilibria of system 6.

binaries, the present LCT theory still needs improvement to predict the critical compositions correctly for ternary system.

For the series of systems 4, 5 and 6, chain lengths are kept as invariants. The reduced exchange interaction-energy parameter between components 2 and 3, $\tilde{\epsilon}_{23}$ is chosen as a variable to study the dependence of the phase equilibria on the interaction energy. The binodals from the computer simulations and those from the Flory−Huggins theory and LCT theory are plotted in Figures 6−8. The immisicible region becomes larger when the energy parameter $\tilde{\epsilon}_{23}$ changes from positive to negative. Similar to Figures 3−5, greater agreement is shown by the LCT theory than by the Flory−Huggins theory. However, large deviations still exist near the critical consolute point.

4. Conclusions

The configuration-bias-vaporation method developed previously has been successfully applied to simulate the liquid−liquid equilibria of ternary chain molecule systems on a lattice. The coexisting phases can be obtained directly at the end of the simulation. The Rosenbluth−Rosenbluth growth method revised by Siepmann et al. is shown to be effective in generating new configurations for polymer systems on lattice.

When we compared available molecular thermodynamic models, including the classical Flory−Huggins theory and the recent LCT theory, as well as modifications such as the revised Freed model by Hu et al.,[19] the behavior near the critical region is not entirely satisfactory. Further effort is needed to model binary and ternary systems near the critical region.

Acknowledgment. This work was supported by the Chinese National Science Foundation (Grant No. 29236130) and the Doctoral Research Foundation of the State Education Commission of China.

References and Notes

(1) Panagiotopoulos, A. Z. *Mol. Phys.* **1987**, *61*, 813. Panagiotopoulos, A. Z.; Quirke, N.; Stapleton, M.; Tildesley, D. J. *Mol. Phys.* **1988**, *63*, 527.
(2) Laso, M.; de Pablo, J. J.; Suter, U. W. *J. Chem. Phys.* **1992**, *97*, 2817.
(3) Madden, W. G.; Pesci, A. I.; Freed, K. F. *Macromolecules* **1990**, *23*, 1181.
(4) Guo, M. X.; Lu, B. C.-Y. *J. ChICRE* **1996**, *27*, 205.
(5) Mackie, A. D.; O'Toole, E. M.; Hammer, D. A.; Panagiotopoulos, A. Z. *Fluid Phase Equilib.* **1993**, *82*, 251.
(6) Harris, J.; Rice, S. A. *J. Chem. Phys.* **1988**, *88*, 1298.

(7) Siepmann, J. I.; Frenkel, D. *Mol. Phys.* **1992**, *75*, 59.
(8) Yan, Q. L.; Liu, H. L.; Hu, Y. *Macromolecules* **1996**, *29*, 4066.
(9) Flory, P. J. *J. Chem. Phys.* **1942**, *10*, 51. Huggins, M. L. *J. Phys. Chem.* **1942**, *9*, 440.
(10) Bawendi, M. G.; Freed, K. F. *J. Chem. Phys.* **1988**, *88*, 2741.
(11) Dudowicz, J.; Freed, K. F. *Macromolecules* **1991**, *24*, 5076; **1995**, *28*, 2276.
(12) Sariban, A.; Binder, K. *J. Chem. Phys.* **1987**, *86*, 5859.
(13) Sariban, A.; Binder, K. *Macromolecules* **1988**, *21*, 711.
(14) Sariban, A.; Binder, K. *Macromolecules* **1991**, *24*, 578.
(15) Sariban, A.; *Macromolecules* **1991**, *24*, 1134.
(16) Deutsch, H. P.; Binder, K. *Macromolecules* **1992**, *25*, 6214.
(17) Rosenbluth, M. N.; Rosenbluth, A. W. *J. Chem. Phys.* **1955**, *23*, 356.
(18) Yan, Q. L.; Jiang, J. W.; Liu, H. L.; Hu, Y. *Chem. Eng. (China)* **1995**, *46*, 517.
(19) Hu, Y.; Liu, H. L.; Shi, Y. H. *Fluid Phase Equilib.* **1996**, *117*, 100.

MA961873+